Structure of the Lipopolysaccharide from the Bradyrhizobium sp ORS285 rfaL Mutant Strain

Flaviana Di Lorenzo, Angelo Palmigiano, Katarzyna A. Duda, Mateusz Pallach, Nicolas Busset, Luisa Sturiale, Eric Giraud, Domenico Garozzo, Antonio Molinaro, Alba Silipo

ChemPubSoc Europe

DOI: 10.1002/open.201700074

Open Access ChemistryOPEN Full Papers

Structure of the Lipopolysaccharide from the *Bradyrhizobium* sp. ORS285 *rfaL* Mutant Strain

Flaviana Di Lorenzo,[a] Angelo Palmigiano,[b] Katarzyna A. Duda,[c] Mateusz Pallach,[a] Nicolas Busset,[d] Luisa Sturiale,[b] Eric Giraud,[d] Domenico Garozzo,[b] Antonio Molinaro,[a] and Alba Silipo*[a]

The importance of the outer membrane and of its main constituent, lipopolysaccharide, in the symbiosis between rhizobia and leguminous host plants has been well studied. Here, the first complete structural characterization of the entire lipopolysaccharide from an O-chain-deficient *Bradyrhizobium* ORS285 *rfaL* mutant is achieved by a combination of chemical analysis, NMR spectroscopy, MALDI MS and MS/MS. The lipid A structure is shown to be consistent with previously reported *Bradyrhizobium* lipid A, that is, a heterogeneous blend of penta- to hepta-acylated species carrying a nonstoichiometric hopanoid unit and possessing very-long-chain fatty acids ranging from 26:0(25-OH) to 32:0(31-OH). The structure of the core oligosaccharide region, fully characterized for the first time here, is revealed to be a nonphosphorylated linear chain with methylated sugar residues, with a heptose residue exclusively present in the outer core region, and with the presence of two singly substituted 3-deoxy-D-*manno*-oct-2-ulosonic acid (Kdo) residues, one of which is located in the outer core region. The lipid A moiety is linked to the core moiety through an uncommon 4-substituted Kdo unit.

1. Introduction

Bradyrhizobia are Gram-negative nitrogen-fixing bacteria capable of establishing a mutualistic symbiotic relationship with plants of the *Leguminosae* family. The endosymbiotic interaction causes the development of root nodules at which bacteria can reduce atmospheric nitrogen into ammonia for the plant's benefit.[1] Owing to their ability to develop a nitrogen-fixing symbiosis, leguminous plants can develop in nitrogen-deficient soil and their culture does not require the addition of nitrogenous chemical fertilizers.[2]

The establishment of this symbiosis relies on an exchange of diffusible signal molecules between the two partners in which lipochitooligosaccharides, termed nodulation factors (Nod factors), synthesized by the bacteria, are essential for controlling the processes of infection and nodule organogenesis. However, Giraud et al. demonstrated that some tropical legumes of the *Aeschynomene* genus, such as *A. indica*, are nodulated by photosynthetic *Bradyrhizobium* strains, such as BTAi1 and ORS278, that lack the canonical *nod*ABC genes responsible for the synthesis of Nod factors.[3] This observation indicated, for the first time, the existence of an alternative symbiotic pathway independent of the Nod factors. Moreover, some photosynthetic *Bradyrhizobium* strains, for example, ORS285, do contain the *nodABC* genes and display a broader host range comprising all stem-nodulating *Aeschynomene* species, including *A. afraspera*. Mutations of the *nod* genes in ORS285 exerted no effects on its ability to nodulate *A. indica*, whereas the ability to nodulate *A. afraspera* was completely abolished. This observation suggested the possibility that strain ORS285 uses distinct symbiotic strategies depending on the host plant, with the involvement of different signal molecules, which remain unidentified.[3]

Exposed on the Gram-negative bacterial surface, lipopolysaccharide (LPS) molecules have an important role in the interaction of bacteria with the host legume.[4,5] LPS is a tripartite macromolecule built up of a glycolipid portion—lipid A—linked to a saccharide part that is distinguished by oligosaccharide (core OS) and polysaccharide portions, the latter being

[a] F. Di Lorenzo, M. Pallach, A. Molinaro, Prof. A. Silipo
Department of Chemical Sciences
University of Naples Federico II
Via Cinthia 4, 80126, Naples (Italy)
E-mail: silipo@unina.it

[b] A. Palmigiano, L. Sturiale, D. Garozzo
CNR-Istituto per i Polimeri
Compositi e Biomateriali IPCB—Unità di Catania
Via Gaifami 18, 95126, Catania (Italy)

[c] K. A. Duda
Junior Group of Allergobiochemistry
Research Center Borstel, Leibniz Center for Medicine and Biosciences
Airway Research Center North (ARCN)
German Center for Lung Research, 23845 Borstel (Germany)

[d] N. Busset, E. Giraud
IRD, Laboratoire des Symbioses Tropicales et Méditerranéennes
UMR IRD/SupAgro/INRA/UM2/CIRAD
Campus International de Baillarguet
TA A-82/J, 34398 Montpellier Cedex 5 (France)

Supporting Information and the ORCID identification number(s) for the author(s) of this article can be found under https://doi.org/10.1002/open.201700074.

termed the O-chain (or O-polysaccharide or O-antigen). Depending on the presence or absence of this latter polysaccharide domain, the LPS macromolecule is defined as smooth-type (S-LPS) or rough-type LPS (R-LPS or lipooligosaccharide, LOS), respectively.[6,7] Although the general architecture of lipid A is conserved among individuals belonging to the same species, lipid As isolated from rhizobia strains are heterogeneous in nature in terms of sugar backbone and lipid content, that is, the nature and distribution of the acyl chains and the presence of very-long-chain fatty acids (VLCFAs).[8] Furthermore, in some bradyrhizobial strains, a triterpenoid moiety, that is, a hopanoid, was found to be covalently linked to the LPS lipid A, and was shown to have a pivotal role in the free living and symbiotic states of the bacteria.[9] The remarkable structural diversity in the lipid A of some rhizobium species is deemed a strategy by which the bacterium can escape or attenuate the plant response, thus facilitating the instauration of symbiosis. The O-chain is the most variable LPS region and is directly involved in the symbiotic interaction with the host plant.[3–5,10] The structural diversity of the O-chain moiety can contribute to modulating or suppressing the plant defense responses.[11] Indeed, it has been observed that the LPS O-polysaccharide from the photosynthetic *Bradyrhizobium* BTAi1a strain, a homopolymer made up of a bicyclic monosaccharide (bradyrhizose),[12] does not trigger the innate immune response in different plant families.[13]

Recently, we have reported two *Bradyrhizobium* ORS285 mutants in the genes *gdh* and *rfaL*, which encode a putative dTDP-glucose 4,6-dehydratase and a putative O-chain ligase, respectively;[14] these mutant strains display an LPS lacking the O-chain moiety. However, no effect of the mutations was detected on the symbiotic properties of these strains regardless of the *Aeschynomene* species considered.[13] This in contrast to many rhizobial species, such as *B. japonicum*, *Rhizobium etli* or *R. phaseoli*, for which the absence of the O-chain is reported to cause a dramatic decrease in symbiotic capacity.[15–17] Thus, the ability of the O-antigen-lacking ORS285 mutants to retain nodulation-promoting properties is not yet fully understood.

In addition to the importance of determining the role of LPS in symbiotic bacteria, rhizobial LPSs have unique structural features not yet fully elucidated. Indeed, all rhizobial core OS characterized to date were found to be completely distinct from enteric LPS, including sugar composition, linkage pattern and absence of phosphate and heptose residues. With regards to the structural features, in the majority of *Agrobacterium* species an α-mannose (α-Man) or α-glucose (α-Glc) moiety is linked to the O-5 atom of the first Kdo unit, with the exception of *Agrobacterium larrymoorei*, in which an α-D-Gal unit is present, whereas in the rhizobium core there are additional galacturonic (GalA) residues, and a third Kdo unit is present in the outer core region.[18–22]

To shed light on the peculiar rhizobial sugar arrangement, we report the structural elucidation of the LPS from the O-chain-deficient *Bradyrhizobium* ORS285 *rfaL* mutant strain (hereafter referred to as ORS285 *rfaL*), obtained by the use of chemical, NMR spectroscopy and mass spectrometry techniques on the entire molecule and on the isolated core OS and lipid A fractions.

2. Results and Discussion

2.1. Extraction, Purification, and Compositional Analysis of ORS285 *rfaL*

The LPS of ORS285 *rfaL* was isolated from dried bacterial pellet by using hot phenol/water.[23] SDS-PAGE analysis[24] revealed the presence in the water phase of an LOS. Intensive steps of purification with DNase, RNase and proteases followed by dialysis, ultracentrifugation and gel filtration chromatography were performed. Compositional analyses[25–27] revealed the occurrence of the following moieties: 6-substituted, 4-substituted and terminal mannose (6-Man, 4-Man, *t*-Man, respectively), 3-substituted 4-*O*-methyl-mannose (3-Man-4Me), terminal galacturonic acid (*t*-GalA), 4-substituted glucose (4-Glc), 6-substituted and 4,6-substituted 2,3-diamino-2,3-dideoxy-D-glucose (referred to here as 4,6-DAG and 6-DAG, respectively), terminal *N*-methylglucosamine (*t*-GlcNMe), 7-substituted D,D-heptose (7-Hep), and 4- and 5-substituted 3-deoxy-D-*manno*-oct-2-ulosonic acids (4-Kdo and 5-Kdo). Furthermore, a GlcNMe-(1→7)-Hep disaccharide and traces of 4-substituted D,D-heptose (4-Hep) were also detected. As further confirmation of the mutation of the *rfaL* gene, no bradyrhizose was detected. Fatty acid analysis[28] revealed the occurrence of 14:0(3-OH), 12:0(3-OH), 12:0, 12:1, and VLCFAs, among which 26:0(25-OH) and 32:0(2,31-2OH), and hopanoid, which is fully consistent with the previously reported data on LPS lipid A fatty acid composition from *Bradyrhizobium*.[8,29]

2.2. Isolation and NMR Structural Characterization of the Core Region of ORS285 *rfaL* LOS

To determine the structure of the ORS285 *rfaL* core OS, mild acid hydrolysis was performed to cleave the acid-labile linkage between the Kdo and the lipid A disaccharide backbone. The water-soluble core OS fraction was isolated in the supernatant after a centrifugation step and further purified by means of ion exchange chromatography. Three main fractions, designated X, Y and Z, were eluted from the column and analyzed by NMR spectroscopy; the ^{1}H NMR spectra are reported in Figure 1.

Each fraction underwent a detailed NMR spectroscopic analysis. Homo- and heteronuclear 2D NMR experiments (DQF-COSY, TOCSY, ROESY, NOESY, ^{1}H–^{13}C HSQC, HMBC and HSQC-TOCSY) were performed to assign all the spin systems and to determine the saccharide sequence. The anomeric configuration of each monosaccharide unit was determined on the basis of the $^{3}J_{H\text{-}1,H\text{-}2}$ coupling constant values attained from the DQF-COSY spectrum, whereas the values of the vicinal $^{3}J_{H,H}$ ring coupling constants allowed the relative configuration of each sugar residue to be assigned. Finally, the combination of information attained from the inter-residue NOE connectivity and heteronuclear long-range correlations, together with methylation analysis, allowed the complete characterization of the core OS from ORS285 *rfaL* LPS.

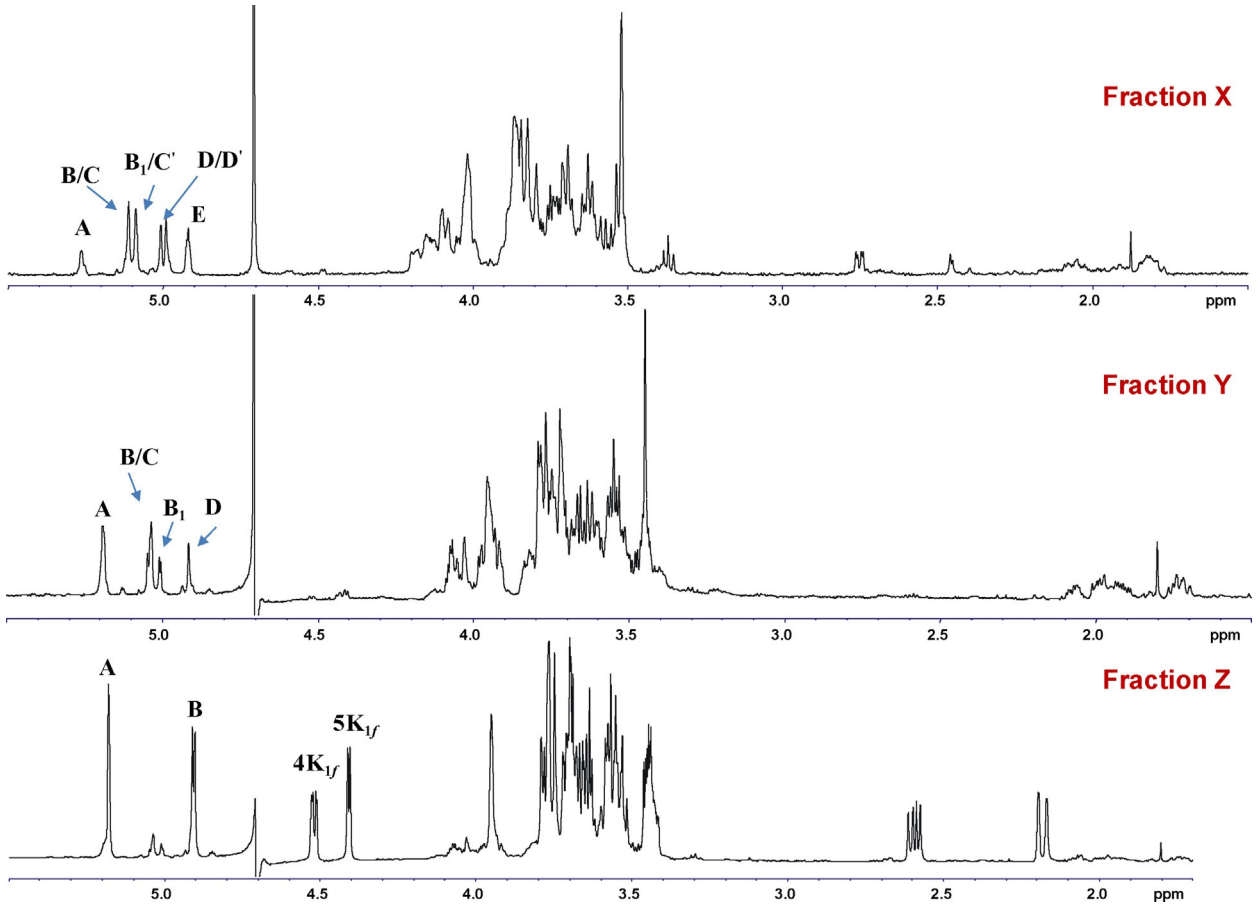

Figure 1. ^{1}H NMR spectra of the ion-exchange chromatography fractions X, Y and Z.

The NMR spectra clearly revealed that fractions X and Y contained a mixture of OS species. Thus, fraction X was composed of three OS species, referred to hereafter as **OS1**, **OS2** and **OS3**. All the sugar residues were present as pyranose rings, according to both ^{13}C chemical shift values and the long-range correlations between C-1/H-1 and H-5/C-5 in the ^{1}H–^{13}C HMBC spectrum (between C-2 and H-6 of the Kdo residue).[30] **OS2** contained spin systems **C**, **D** and **K$_2$** (Table 1 and Figure 1). Spin system **C** (H-1 at 5.11 ppm, Table 1) and was identified as an α-*manno*-configured sugar unit due to the low-value coupling constants $^{3}J_{H\text{-}1,H\text{-}2}$ and $^{3}J_{H\text{-}2,H\text{-}3}$ (< 1 Hz), diagnostic of an H-2 equatorial orientation. Furthermore, in the TOCSY spectrum, it was possible to assign all the other ring protons resonances from H-2, allowing identification of this sugar as a heptose residue. Similarly, spin system **D** (H-1 at 5.01 ppm, Table 1) was identified as an α-mannose moiety due to the $^{3}J_{H\text{-}1,H\text{-}2}$ and $^{3}J_{H\text{-}2,H\text{-}3}$ values of 3 Hz and the intra-residual NOE contact of H-1 only with H-2. Moreover, the downfield shift of C-4 **D** (76.3 ppm, Table 1 and Figure 2) was attributed to the presence of a methoxy group as demonstrated by the NOE correlation of the signal at $\delta = 3.51$ ppm (Table 1) with the signal for H-4 of α-mannose **D** at $\delta = 3.56$ ppm (Table 1); this was further confirmed by the occurrence of a long-range correlation, observed in the ^{1}H–^{13}C HMBC spectrum, between C-4 of **D** and the methoxy group. Finally, spin system **K$_2$** was attributed to the Kdo residue on the basis of the diastereotopic methylene proton signals resonating in the high-field region of the ^{1}H NMR spectrum at $\delta = 1.81$ (H-3$_{ax}$) and 2.05 ppm (H-3$_{eq}$; Table 1); on the basis of the H-3 proton chemical shift it was possible to assign its α-anomeric configuration.[31] Upfield-shifted carbon signals were pivotal in identifying substitution at O-3 of residue **D** and at O-5 of the Kdo unit, whereas residue **C** was assigned to a terminal sugar unit, in agreement with the methylation data. The primary sequence of the **OS2** structure was inferred by using the NOE connectivity measured in the ROESY spectra and by the long-range correlations in the HMBC spectrum (Figure 2). Thus, the Kdo residue **K$_2$** was found to be substituted at its O-5 position by the α-Man4Me **D**, which in turn was substituted at position O-3 by the α-heptose **C**; these data allowed us to define **OS2** as the following trisaccharide (where *p* stands for pyranose) [Eq. (1)]:

OS2

C **D** **K$_2$**

α-Hep*p*-(1→3)-α-Man4Me*p*-(1→5)-Kdo*p*

As stated above, the NMR analysis revealed the presence, in fraction X, of a further OS species, **OS1**. This was identified as a tetrasaccharide (Table 1 and Figures 1 and 2) made up of spin systems **K$_2$**′, **D**′, **C**′ and an extra sugar unit (**E**) compared

Table 1. ^{1}H and ^{13}C chemical shift values [ppm] of fraction X.

Fraction X

OS1/OS2: **E** α-GlcN-(1→7)-α-Hep-(1→3)-α-Man4Me-(1→5)-Kdo*p* (**C/C'**, **D/D'**, **K$_2$/K'$_2$**)

OS3: **A** α-Man-(1→4)-α-Glc-(1→4)-Kdo*p* (**B/B$_1$**, **K$_1$/K'$_1$**)

	1	2	3	4	5	6	7	8
				OS3				
A	5.27/5.26 $^{3}J_{H-1,H-2}$ = 1.6/1.4 Hz	4.028	3.78	3.63	3.66/3.57	3.74/3.82	–	–
t-α-Man	101.46 $^{1}J_{C-1,H-1}$ = 174.2 Hz	70.34	70.38	66.20	73.68	60.58	–	–
B	5.12 $^{3}J_{H-1,H-2}$ = 3.9 Hz	3.54	3.84	3.61	3.90	3.73/3.85	–	–
4-α-Glc	98.3 $^{1}J_{C-1,H-1}$ = 170.5 Hz	71.62	70.70	76.06	70.82	60.60	–	–
B$_1$	5.08 $^{3}J_{H-1,H-2}$ = 3.37 Hz	3.52	3.88	3.60	3.90	3.83/3.75	–	–
4-α-Glc	99.76 $^{1}J_{C-1,H-1}$ = 170.6 Hz	71.63	70.68	76.22	70.81	60.60	–	–
K$_1$/K'$_1$	–	–	2.07 1.77/(2.14)	4.02	3.98/4.10	3.68	–	–
4-α-Kdo*p*			37.41	78.80	70.19	71.90	–	–
				OS1/OS2				
C	5.11 $^{3}J_{H-1,H-2}$ < 1 Hz	4.02	3.86	3.85	3.69	3.69	3.63	–
t-α-Hep	102.02 $^{1}J_{C-1,H-1}$ = 171.2 Hz	70.30	70.64	66.21	72.30	72.15	62.82	–
C'	5.08 $^{3}J_{H-1,H-2}$ < 1 Hz	4.01	3.87	3.86	3.873	4.18	3.69/3.78	–
7-α-Hep	102.09 $^{1}J_{C-1,H-1}$ = 172.4 Hz	70.36	70.60	66.21	70.62	67.49	69.17	–
D/D'	5.01/4.99 $^{3}J_{H-1,H-2}$ < 1 Hz	4.08/4.10	4.02/4.04	3.56/3.54	3.85	3.74	–	–
3-α-Man	101.76 $^{1}J_{C-1,H-1}$ = 174.1 Hz	70.11/70.25	77.21/78.76	76.3/76.00 OCH_3 3.51/60.23	72.33	60.60	–	–
E	4.92 $^{3}J_{H-1,H-2}$ = 3.36 Hz	2.74	3.58	3.37	3.69	3.83/3.74	–	–
t-α-GlcN	98.97 $^{1}J_{C-1,H-1}$ = 170.4 Hz	54.88	73.81	69.80	72.06	60.61	–	–
K$_2$	–	–	1.81/2.05	4.15	3.88	3.85	4.00	3.63/3.80
5-α-Kdo*p*	–	–	37.70	70.80	79.90	72.31	68.91	62.90
K'$_2$	–	–	1.81/1.90	4.14	3.85	3.85	4.00	3.63/3.80
5-α-Kdo*p*	–	–	37.62	69.53	80.58	72.31	68.90	62.90

to **OS2**. Residue **E** (H-1 at 4.92 ppm; Table 1) was identified as α-GlcN: the *gluco* configuration was assigned from the $^{3}J_{H,H}$ coupling constants, whereas the C-2 signal at 54.88 ppm (Table 1) indicated it to be a nitrogen-bearing carbon atom. The analysis of the inter-residual NOE correlations and long-range contacts allowed the location of residue **E** to be identified at position O-7 of the α-heptose **C'** as a terminal sugar unit (Figures 1 and 2). Therefore, **OS1** corresponded with the following tetrasaccharide [Eq. (2)]:

OS1

E **C'** **D'** **K$_{2'}$**

α-GlcN*p*-(1→7)-α-Hep*p*-(1→3)-α-Man4Me*p*-(1→5)-Kdo*p*

OS3 was composed of spin systems **A**, **B** and **K$_1$**. Spin system **A** was identified as an α-mannose, whereas residue **B** was assigned as an α-glucose moiety, as demonstrated by the large ring $^{3}J_{H,H}$ coupling constants, and **K$_1$** was identified as a Kdo unit. The analysis of the glycosylation shifts allowed the identification of **A** as a terminal mannose, of **K$_1$** as a 4-substituted Kdo and of **B** as a 4-substituted glucose unit. The long-range and NOE correlations allowed the elucidation of the following trisaccharide structure [Eq. (3)]:

OS3

A **B** **K$_1$**

α-Man*p*-(1→4)-α-Glc*p*-(1→4)-Kdo*p*

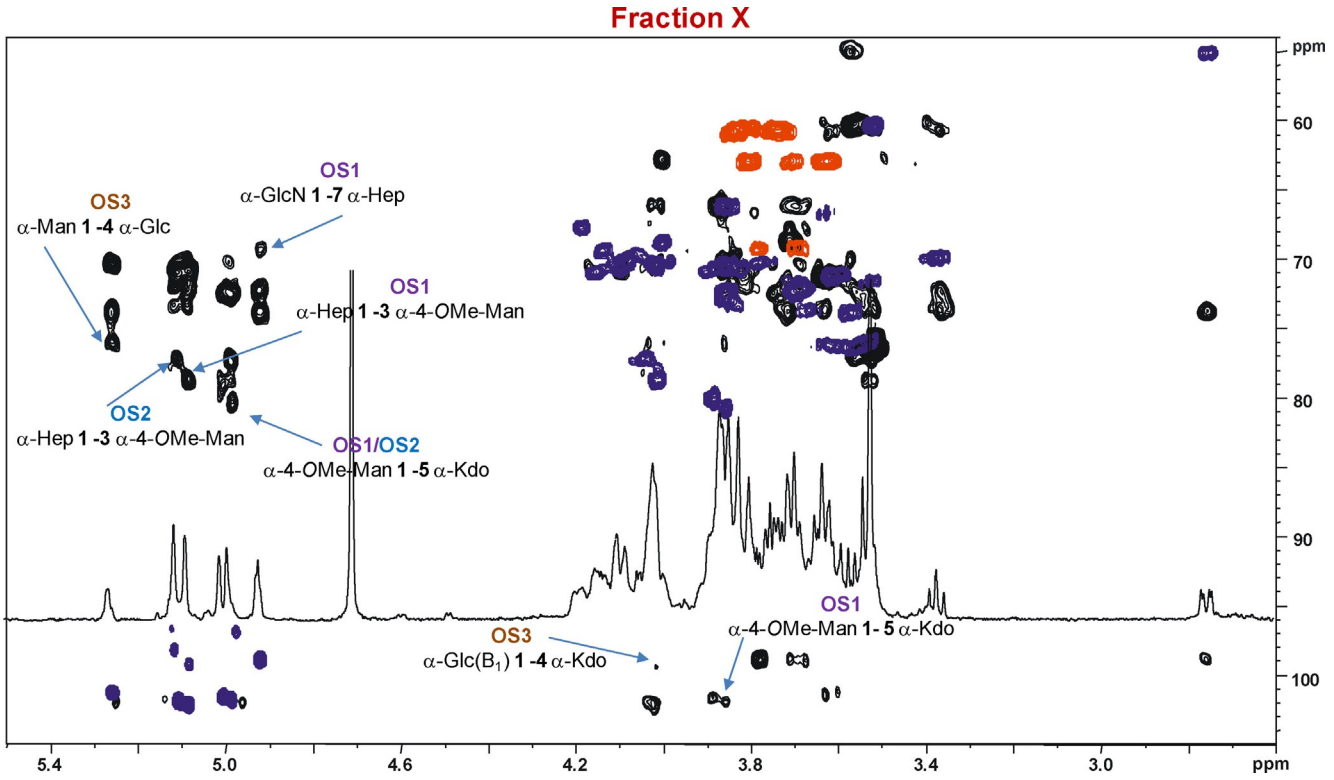

Figure 2. Zoom-in of the overlapped ^{1}H, ^{1}H–^{13}C HMBC (black) and ^{1}H–^{13}C HSQC (purple and red) NMR spectra of the fraction X; the key inter-residual long-range correlations involving sugar moieties are indicated; letters are as in Table 1.

Fraction Y (Figures 1 and 3, Table 2) was exclusively constituted by the **OS2** and **OS3** oligosaccharides described above, and was assigned as above. Fraction Z (Figures 1 and 4) was exclusively composed of **OS3′**, even though the Kdo unit $\mathbf{K_{1f}}$ was present in a furanose form, as demonstrated by long-range correlation of C-2 with H-5, and further confirmed by the chemical shift values (typical of furanose rings) of H-3_{ax} and H-3_{eq} resonating at 2.17/2.59 ppm, C-2 (105.0 ppm) and C-5 (82.3 ppm) (Table 3 and Figure 4).

Thus, according to NMR and compositional analyses, the core OS isolated from *Bradyrhizobium* ORS285 *rfaL* was comprised of two different Kdo-containing oligosaccharide skeletons, a tri/tetrasaccharide with the structure GlcN-(1→7)-Hep-(1→3)-4-*O*Me-Man-(1→5)-Kdo and a trisaccharide having the structure Man*p*-(1→4)-Glc*p*-(1→4)-Kdo*p*.

2.3. MALDI Mass Spectrometry on Intact LOS from ORS285 *rfaL*

An aliquot of intact LOS isolated from ORS285 *rfaL* was investigated by MALDI MS and MS/MS to determine the structure of both lipid A and core domains. The MALDI mass spectrum of intact LOS, recorded in linear mode and with positive-ion polarity, is reported in Figure 5. These data show, in addition to an array of molecular ions, the heterogeneity of the native LOS (*m/z* 3600–4800). In-source decay fragments originated from cleavage (β-elimination) of the labile glycosidic bond involving the Kdo unit to yield either core OS ions (B-type ions, *m/z* 900–1500) and lipid A ions (Y ions, *m/z* 2400–3200).[32,33] Four main oligosaccharide species at *m/z* 1469.6 ($\mathbf{OS_a}$), 1308.5 ($\mathbf{OS_b}$), 1294.5 ($\mathbf{OS_c}$) and 925.4 ($\mathbf{OS_d}$) were clearly identified, together with their corresponding ions arising from the well-known neutral loss of CO_2 ($\Delta m/z$ 44).[32] To obtain the sequence of all these OS structures, we performed the MALDI-TOF MS on intact LOS in the reflectron mode, followed by MALDI-TOF/TOF MS/MS analysis of the related fragments (Figure 6a) produced directly by the LOS fragmentation. In fact, they are MS^3 spectra acquired with a MS/MS instrument,[34] as the precursor ions are B-type fragments originated from the rapid in-source decay of the LOS pseudomolecular ions.

In detail, the peak at *m/z* 1469.6 ($\mathbf{OS_a}$) was consistent with a B-ion matching with an octasaccharide composed of two Kdo, two hexose (Hex), one methyl hexose (HexMe), one heptose (Hep), one hexosamine (HexN) and one methylhexosamine (HexNMe) units (Figure 5). Its fragmentation pattern (Figure 6a) showed numerous informative ions, such as those at *m/z* 1294.5, due to the loss of a terminal Kdo, at *m/z* 925.4, which matches with a fragment lacking one Kdo and two Hex, and at *m/z* 705.3, corresponding to an ion deprived of a further Kdo residue. Finally, the internal fragment at *m/z* 530.3 was indicative of a trisaccharide made up of one HexMe, one Hep and one Hex moiety. The OS species at *m/z* 1308.5 ($\mathbf{OS_b}$) was assigned to a heptasaccharide sharing the same sequence—with the exception of a terminal HexN monosaccharide ($\Delta m/z$ 161)—with $\mathbf{OS_a}$, as confirmed by MS/MS analysis. Similarly, the species at *m/z* 1294.5 ($\mathbf{OS_c}$) was ascribed to a hepta-

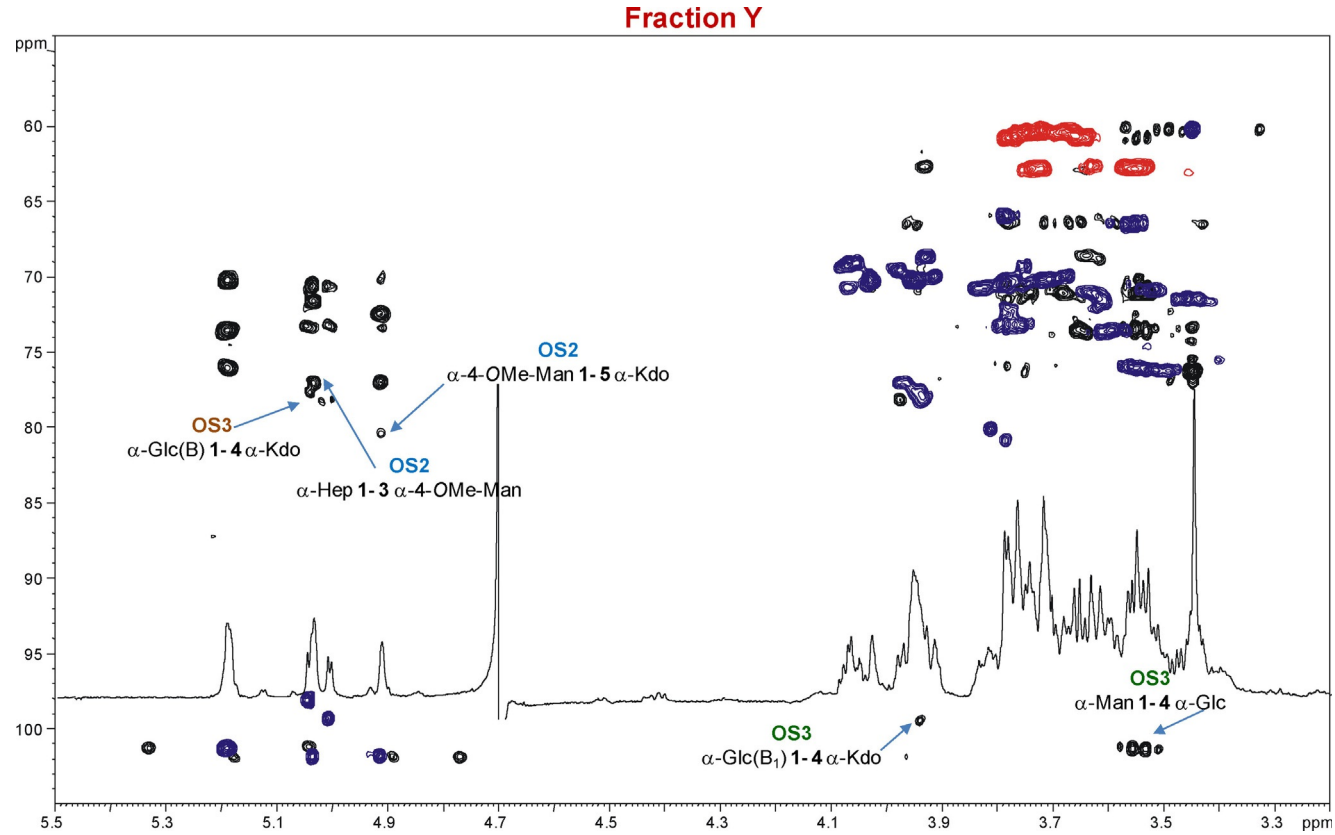

Figure 3. Zoom-in of the overlapped ^{1}H, ^{1}H–^{13}C HMBC (black) and ^{1}H–^{13}C HSQC (purple and red) NMR spectra of the fraction Y; the key inter-residual long-range correlations involving sugar moieties are indicated; letters are as in Table 2.

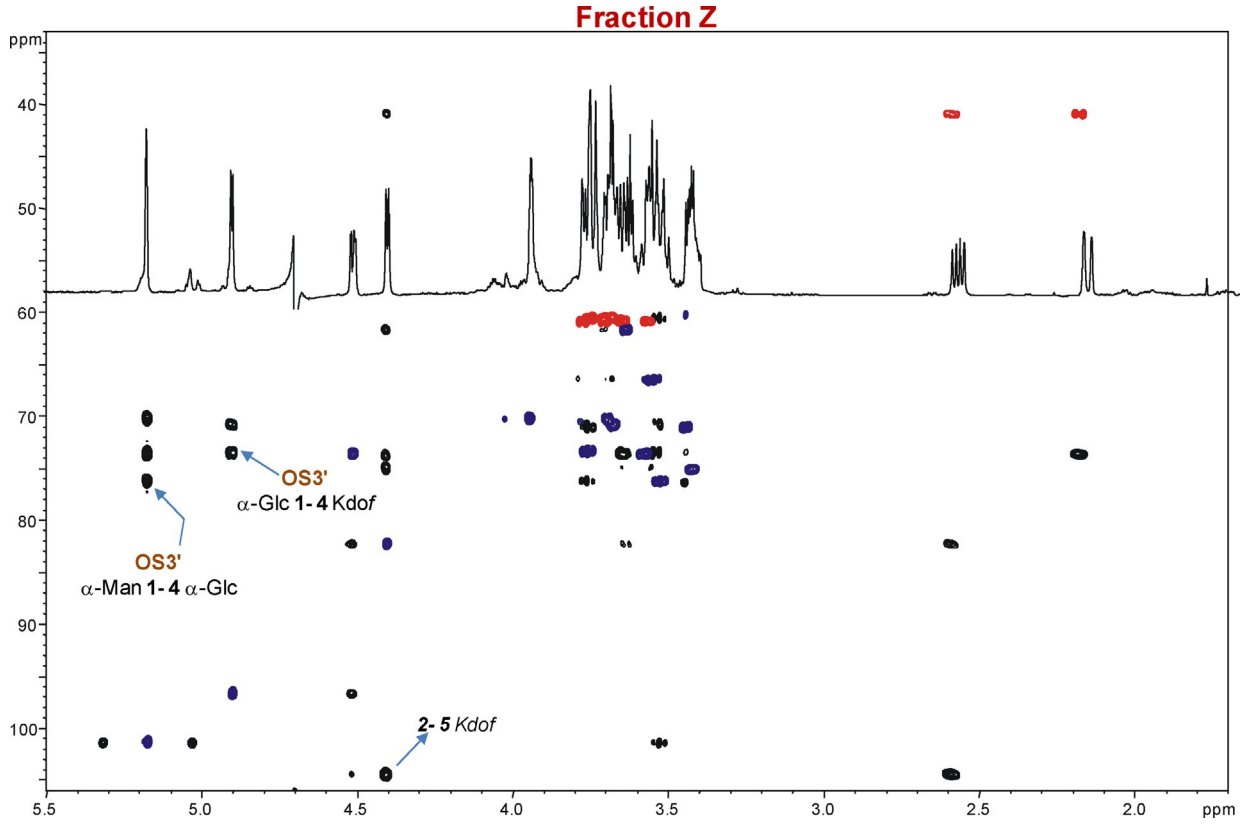

Figure 4. Zoom-in of the overlapped ^{1}H, ^{1}H–^{13}C HMBC (black) and ^{1}H–^{13}C HSQC (purple and red) NMR spectra of the fraction Z; the key inter-residual long-range correlations involving sugar moieties are indicated; letters are as in Table 3.

Table 2. ^{1}H and ^{13}C chemical shift values [ppm] of fraction Y.

Fraction Y

OS2: C α-Hep-(1→3)-α-Man4Me-(1→5)- D Kdop K_2/K'_2

OS3: A α-Man-(1→4)-α-Glc-(1→4)-Kdop B/B_1 K_1/K'_1

	1	2	3	4	5	6	7	8
				OS3				
A	5.18 $^{3}J_{H-1,H-2}=1.92$ Hz	3.96	3.71	3.568	3.60	3.77/3.64	–	–
t-α-Man	101.35 $^{1}J_{C-1,H-1}=174.3$ Hz	70.26	70.17	66.53	73.60	60.76	–	—
B	5.04 $^{3}J_{H-1,H-2}=3.9$ Hz	3.47	3.78	3.56	3.83	3.71	–	–
4-α-Glc	98.15 $^{1}J_{C-1,H-1}=170.3$ Hz	71.60	73.24	76.09	70.30	60.38	–	–
B_1	5.01 $^{3}J_{H-1,H-2}=3.85$ Hz	3.44	3.75	3.53	3.83	3.68	–	–
4-α-Glc	99.4 $^{1}J_{C-1,H-1}=170.2$ Hz	71.60	73.26	76.20	70.60	60.38	–	–
K_1	–		1.71/1.99	3.94	4.06	–	–	–
4-α-Kdop			36.10	77.91	70.5	–	–	–
K'_1	–		1.99	3.95	3.91	–	–	–
4-α-Kdop			36.11	77.8	69.92	–	–	–
				OS2				
C	5.03 $^{3}J_{H-1,H-2}<1$ Hz	3.94	3.79	3.79	3.75	3.67	3.62	–
t-α-Hep	102.00 $^{1}J_{C-1,H-1}=173.0$ Hz	70.31	70.50	65.80	73.00	71.15	62.62	–
D	4.91 $^{3}J_{H-1,H-2}<1$ Hz	4.02	3.97	3.48	3.77	3.67	–	–
3-α-Man	101.7 $^{1}J_{C-1,H-1}=171.2$ Hz	70.18	77.01	76.18	72.1	60.30	–	–
				OCH_3 3.45/60.23				–
K_2	–	–	1.74/1.98	4.06	3.81	3.78	3.93	3.63/3.73
5-α-Kdop	–	–	37.17	69.2	80.30	70.42	68.70	62.80
K'_2	–	–	1.73/1.82	3.98	3.78	3.78	3.93	3.63/3.73
5-α-Kdop	–	–	37.60	69.41	80.92	70.41	68.70	62.80

Table 3. ^{1}H and ^{13}C chemical shift values [ppm] of fraction Z.

Fraction Z

OS3': A α-Man-(1→4)-α-Glc-(1→4)-Kdof B K_{1f}

	1	2	3	4	5	6	7	8
A	5.17 $^{3}J_{H-1,H-2}=1.31$ Hz	3.95	3.69	3.56	3.58	3.78/3.64	–	–
t-α-Man	101.41 $^{1}J_{C-1,H-1}=177.0$ Hz	70.18	70.28	66.5	73.6	60.84	–	–
B	4.90 $^{3}J_{H-1,H-2}=1.31$ Hz	3.44	3.75	3.53	3.69	3.67/3.75	–	–
4-α-Glc	96.60 $^{1}J_{C-1,H-1}=170.9$ Hz	70.98	73.39	76.04	70.18	60.50	–	–
K_{1f}	–	–	2.17/2.59	4.52	4.41	3.63	3.43	3.71/3.56
4-α-Kdof	173.0	105.00	41.00	73.40	82.34	61.50	75.06	60.74

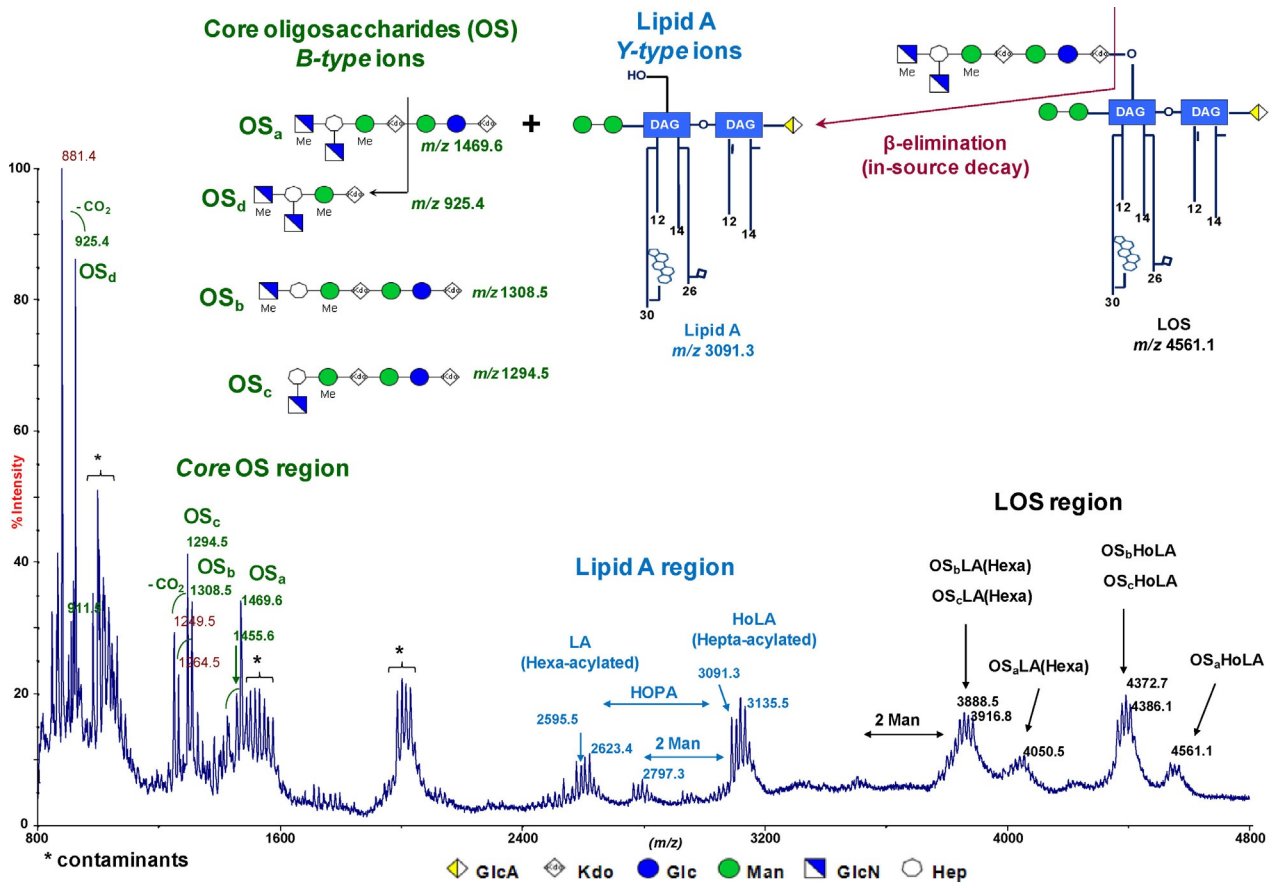

Figure 5. Linear MALDI-TOF mass spectrum in positive-ion mode of intact LOS from *Bradyrhizobium* ORS285 *rfaL*. Pseudomolecular ions are present in the LOS region. Further peaks are due to in-source fragmentation as sketched for the LOS species at *m/z* 4561.1. * Indicates contaminants.

saccharide consisting of the same **OS$_a$** sequence lacking a terminal HexNMe (Δ*m/z* 175). Finally, the B-ion at *m/z* 925.4 (**OS$_d$**) was identified as a pentasaccharide made up of one Kdo, one MeHex, one Hep, one HexN and one HexNMe residue, derived from the longer octasaccharide species (**OS$_a$**) at *m/z* 1469.6, as a result of the rupture of the labile glycosidic bond involving the intra-chain Kdo unit. The MS/MS analysis of **OS$_d$** showed two pairs of intense ions at *m/z* 162.1 and 764.3 and at *m/z* 176.1 and 750.3, corresponding to B- and Y-type ions obtained from the loss of a terminal HexN and a terminal HexNMe, respectively. Moreover, the internal fragment at *m/z* 530.2 and a further fragment at *m/z* 529.2 support the presence of a Hep unit substituted by two HexN residues, of which one is methylated, as outlined in Figure 6a. Indeed, the occurrence of minor OS peaks at *m/z* 1455.6 and 911.5 (Δ*m/z* 14) implied that the methylation on the HexN residue was nonstoichiometric (Figure 5).

We were unable to locate, either by NMR or GC–MS, the second HexN unit, although traces of 4-Hep in the methylation analysis might lead us to conclude that the second amino sugar is located at this position. Conversely, the finding of a 4-Man residue in the methylation analysis allowed us to establish that the second Kdo unit was located at position 4 of the α-mannose. Indeed, data obtained from methylation, MS and NMR analyses led us to propose the following structure for the main core **OS$_b$** (Figures 5 and 7): α-GlcNMe-(1→7)-α-Hep-(1→3)-α-Man4Me-(1→5)-α-Kdo-(2→4)-α-Man-(1→4)-α-Glc-(1→4)-α-Kdo.

Figure 5 shows, in the mass range between *m/z* 2400 and 3200, a series of peaks relative to the heterogeneous mixture of lipid A species differing in their acylation pattern, that is, in the lipid chain nature and content. The complete assignment of the lipid A fraction was achieved in detail by MS analysis in reflectron mode on intact LOS. A zoom-in view of this latter spectrum enclosing the lipid A region, is reported in Figure S1. In brief, a penta-acylated lipid A species was identified at lower masses (*m/z* 2128.39), composed of a pentasaccharide backbone, constituted by a disaccharide of DAG units carrying an α-Gal*p*A on the vicinal DAG and an α-Man*p* disaccharide on the distal DAG unit, acylated by two 14:0(3-OH), one 12:0(3-OH), one 12:1, and one acetylated 26:0(25-OAc) moiety. A second group of peaks was ascribed to the hexa-acylated lipid A fraction with the same acylation pattern plus a VLCFA, the major component of which ranged from C30:0(29-OH) to C32:0(2,31-2OH), in full agreement with previously published lipid A structure from *B. japonicum* strain BTAi1.[8] A third group of lipid A peaks were found shifted to higher molecular mass by Δ*m/z* 512.4, thus suggesting the presence of a hopanoid moiety, once more in accordance with previous reported data on *Bradyrhizobium* lipid A.[8] The MS/MS analysis on a single Y-

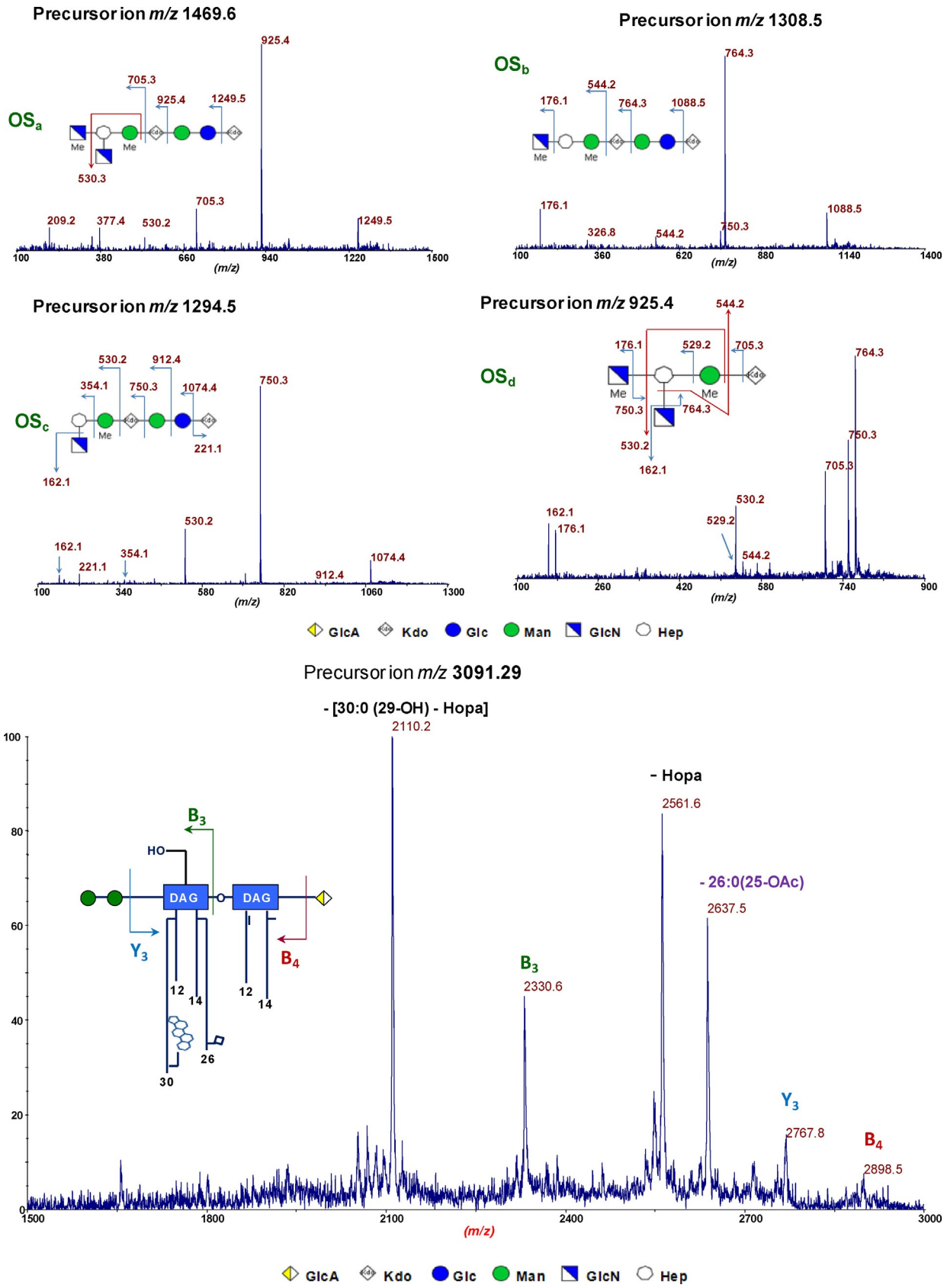

Figure 6. a) MALDI-TOF/TOF MS/MS analysis of the main OS species (B-type ions) generated in-source over the MALDI-TOF acquisition. b) MALDI-TOF/TOF MS/MS analysis of the lipid A species (Y-type ion) at *m/z* 3091.29, generated in-source over the MALDI-TOF acquisition. Assignments of the fragment ions are shown on the schematic structures.

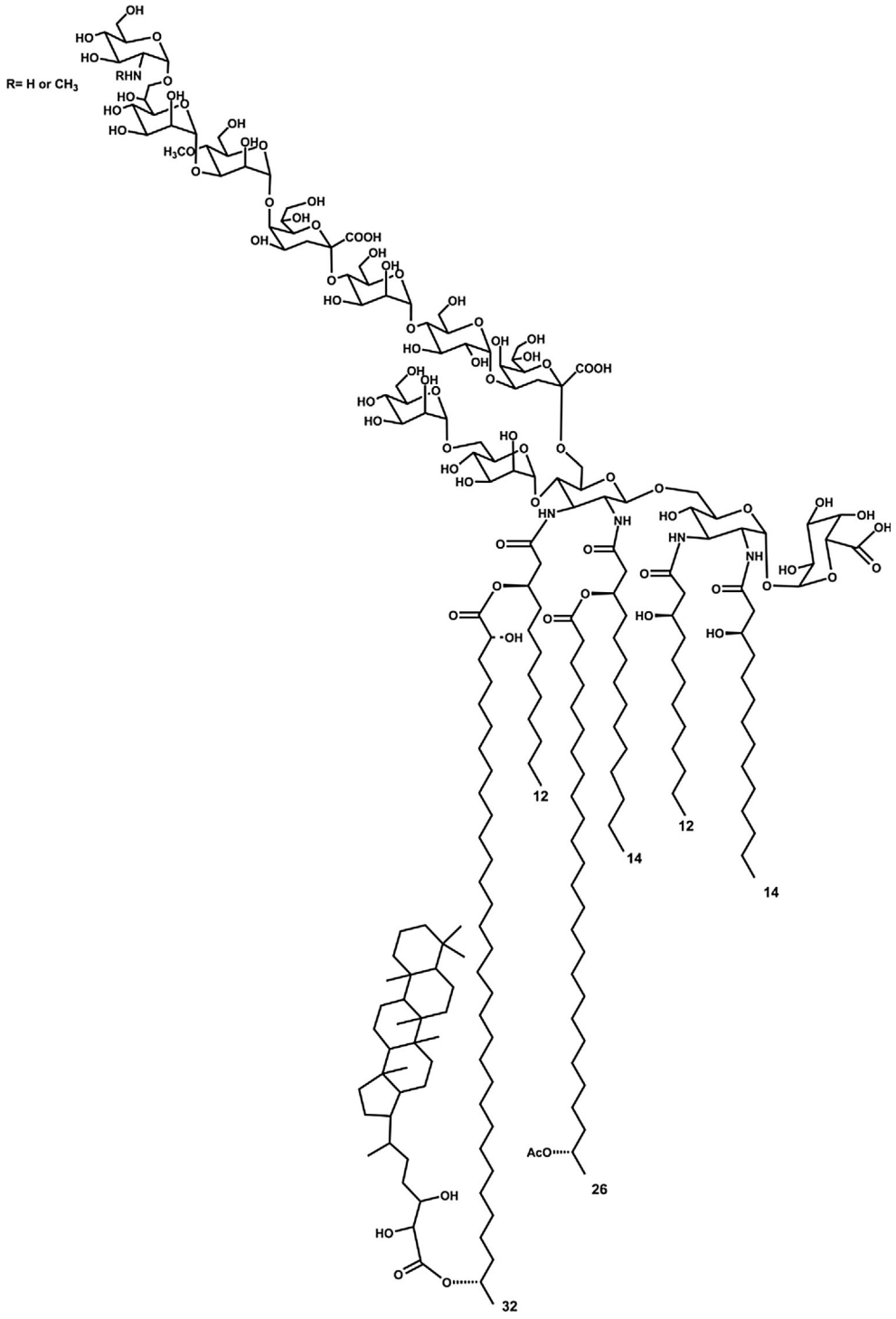

Figure 7. Complete structure of the LPS from the ORS285 *rfaL* mutant strain. MALDI MS data highlighted the presence of a second amino sugar linked to the heptose residue.

type ion allowed full characterization of the hepta-acylated lipid A species at *m/z* 3091.29, as reported in Figure 6b.

Finally, heterogeneous groups of ions corresponding to the native LOS, given by the combination of all the full-length core OS species (namely $\mathbf{OS_a}$, $\mathbf{OS_b}$ and $\mathbf{OS_c}$) and the main lipid A moieties, were detected at higher molecular masses (*m/z* 3600–4800), as shown in Figure 5.

3. Conclusions

Bradyrhizobia are symbiotic bacterial partners that develop nitrogen-fixing nodules in a large diversity of leguminous species.[1] Root colonization is a key step in the interaction of these beneficial bacteria with plants,[35] thus the molecular mechanisms involved in such a delicate process have attracted increasing interest in several research fields. It was previously

reported that the bacterial outer membrane is involved in most of the host–microbe interactions, and consequently the LPS, as the main component of the outer membrane, is considered one of the primary actors potentially involved in the symbiotic process. In this context, several works suggested the importance of the LPS both in the very early recognition steps with the host and in the later stages of the nodulation processes,[3,4,36] focusing the attention on the role of the LPS O-chain moiety, presence of which is considered a pivotal prerequisite for a successful plant–microbe interaction at different stages of the nodulation event. Nevertheless, through the analysis of *Bradyrhizobium* ORS285 mutant strains lacking the LPS polysaccharide domain, we have recently demonstrated that the O-chain of *Bradyrhizobium* strains is not required for establishing symbiosis with *Aeschynomene* spp.[13] The reason for such peculiar behavior is unresolved. However, the existence of as yet unknown symbiotic processes cannot be excluded. The possibility that the core OS region, as the outermost part of the *Bradyrhizobium* ORS285 mutants LPS, can be non-immunogenic and thus facilitate symbiosis, is also an important issue to be considered. This hypothesis prompted us to elucidate the complete structure of the LOS from the *Bradyrhizobium* ORS285 *rfaL* mutant.

The structural characterization of the core OS and lipid A was enabled by the combination of chemical, MS, MS/MS, and NMR analyses on both native LOS and its isolated constituents. The core OS region isolated from ORS285 *rfaL* is heterogeneous in terms of sugar composition, as observed from NMR and MS data, and consists of a mixture of hepta- and octa-saccharide species containing 1) a trisaccharide with the structure α-Man-(1→4)-α-Glc-(1→4)-α-Kdo, and 2) a tetrasaccharide having the structure α-GlcN-(1→7)-α-Hep-(1→3)-α-4*O*MeMan-(1→5)-α-Kdo, with the α-GlcN unit present in a nonstoichiometric amount. In addition, MS analyses showed the existence of a further GlcN unit linked to the heptose residue; furthermore, neither GlcN unit was stoichiometrically N-methylated. The heterogeneity of the native LOS was also clearly visible in the high-mass region of the MALDI MS spectrum (*m/z* 4100–4600, Figure 5), from which different species were identified differing in the acylation pattern of the lipid A, the length, and extent of methylation of the core region. Moreover, the lipid A component of intact LOS was fully characterized by HRMS in the reflector mode (Figure S1) and MS/MS analysis of the Y-type ions generated by in-source decay (Figure 6b). The elucidated structure was fully consistent with that previously published for *Bradyrhizobium* strains, that is, a mixture of penta- to hepta-acylated species carrying a nonstoichiometric hopanoid residue and both possessing two 14:0(3-OH), two 12:0(3-OH), and two VLCFAs, for example, one 26:0(25-OAc) and one VLCFA ranging from 26:0(25-OH) to 32:0(31-OH).[8]

Notably, this is the first complete structure of *Bradyrhizobium* LPS lipid A core region; previously, only partial structures were reported.[37] With regard to our finding, the core moiety of ORS285 *rfaL* is revealed to be a new core oligosaccharide with somewhat unique structural features. In brief, ORS285 *rfaL* LOS displayed 1) a linear core oligosaccharide chain containing two Kdo residues, and 2) one of the two Kdo residues is placed four residues away from the lipid A domain, that is, in the outer core region of the LOS, and represents a structural feature in common with other rhizobial species, in which a Kdo unit was found in the O-chain attachment region.[18–22,38] Moreover, no phosphate groups decorating such a core OS region were detected. As a further peculiarity, the lipid A sugar backbone is connected to the core region through a 4-substituted Kdo residue, whereas, in the majority of core structures characterized so far, the first Kdo is 5-monosubstituted or 4,5-disubstituted. Finally, the occurrence of methylated sugar residues comprising the ORS285 *rfaL* LOS is a further characteristic in common with other *Bradyrhizobium* core OS moieties. In other rhizobial strains, sugar methylation has been correlated to the switch to an increase in the surface hydrophobicity from a predominantly hydrophilic state.[10,39,40] It has been also hypothesized that, together with the features of lipid A—the presence of VLCFA and hopanoid moieties—the presence of methylated sugar units can further contribute to increased bacterial envelope stability and barrier properties as well as bacterium adhesion ability, for example, that facilitating plant–microbe interactions.

Experimental Section

Bacterial Strain and LPS Isolation

Dried cells were washed twice with distilled water and extracted with a hot phenol/water mixture.[17] After extensive dialysis against distilled water, the extracted phases underwent enzymatic digestion and an ultracentrifugation step in order to remove nucleic acid and protein contaminants. Both fractions were analyzed by SDS-PAGE (13.5% acrylamide) followed by silver nitrate staining.[18] In order to remove glucan contaminants, a phenol/chloroform/light petroleum extraction,[41] followed by a precipitation step with cold acetone, was performed.

Structural Analysis of LOS from ORS285 *rfaL*

The structure of the LOS from ORS285 *rfaL* was characterized using a range of methods. Monosaccharides were detected as acetylated *O*-methylglycoside derivatives obtained by methanolysis (1.25 M HCl/MeOH, 85 °C, 24 h) followed by acetylation with acetic anhydride in pyridine (85 °C, 30 min).[19] Linkage analysis was performed as previously described.[20,21] In brief, the sample was methylated with iodomethane and hydrolyzed with trifluoroacetic acid (2 M, 100 °C, 2 h). The carbonyl was reduced with sodium tetradeuteroborate ($NaBD_4$), then the sample was acetylated with acetic anhydride and pyridine, and analyzed by GLC–MS.

After hydrolysis of the LOS (4 M HCl, 100 °C, 4 h), neutralization (5 M NaOH, 100 °C, 30 min) and water/chloroform extraction, fatty acids were detected in the chloroform phase by gas–liquid chromatography [HP 6890 N gas chromatograph with flame ionization detection and an Agilent Technologies column (30 m × 0.25 mm, film thickness 0.25 μm) of phenyl methylsiloxane HP-5MS] as methyl esters (diazomethane, 10 min, room temperature).[28] The temperature program was 120 °C for 3 min, then heating to 320 °C at 5 °C min^{-1}.

Isolation of the ORS285 *rfaL* LOS Constituents

To study the core OS component, a portion (20 mg) of purified LOS was treated with acetate buffer (pH 4.4) for 5 h at 100 °C with magnetic stirring. An appropriate mixture of chloroform and methanol was added to the hydrolysate to obtain a chloroform/methanol/hydrolysate (2:2:1.8, *v*/*v*/*v*) mixture. The mixture was then shaken and centrifuged. The water-soluble phase, containing the core OS fraction, was collected and freeze-dried. This fraction was then purified by high-performance anion-exchange chromatography coupled with pulsed amperometric detection (HPAEC-PAD) in alkaline conditions. Later, the samples were desalted by gel permeation chromatography on a G-10 column (GE Healthcare).

NMR Spectroscopy Analysis

1D and 2D NMR spectra were recorded in D_2O at 27 °C at pD 7 with a cryoprobe-equipped Bruker 600 DRX spectrometer. Total correlation spectroscopy (TOCSY) experiments were performed with spinlock times of 100 ms using data sets ($t1 \times t2$) of 4096×512 points. Rotating-frame Overhauser enhancement spectroscopy (ROESY) and nuclear Overhauser enhancement spectroscopy (NOESY) experiments were performed using data sets ($t1 \times t2$) of 4096×512 points with mixing times between 100 and 400 ms. Double-quantum-filtered phase-sensitive correlation spectroscopy (DQF-COSY) experiments were performed using data sets of 4096×912 points. The data matrix in all homonuclear experiments was zero-filled in both dimensions to give a matrix of 4 K×2 K points, and was resolution-enhanced in both dimensions using a cosine-bell function before Fourier transformation. Coupling constants were determined by 2D phase-sensitive DQF-COSY measurments.[42,43] Heteronuclear single-quantum coherence (HSQC) and heteronuclear multiple-bond correlation (HMBC) experiments were performed in the ^{1}H-detection mode by single-quantum coherence with proton decoupling in the ^{13}C domain using data sets of 2048×400 points. HSQC was performed using sensitivity improvement and in the phase-sensitive mode using echo/antiecho gradient selection, with multiplicity editing during the selection step.[44] HMBC was optimized on long-range coupling constants, with a low-pass *J* filter to suppress one-bond correlations, using gradient pulses for selection. Moreover, a 60 ms delay was used for the evolution of long-range correlations. HMBC spectra were optimized for 6–15 Hz coupling constants. The data matrix in all the heteronuclear experiments was extended to 2048×1024 points by using a forward linear prediction extrapolation.[45]

MALDI-TOF and MALDI-TOF/TOF Mass Spectrometry

A 4800 Proteomic Analyzer (AB Sciex) was used, equipped with a Nd:YAG laser operating at a wavelength of 355 nm with a $<$500 ps pulse and 200 Hz firing rate. MALDI-TOF mass spectra of intact LOS were recorded either in linear or reflectron mode using positive-ion polarity. Each spectrum resulted from the sum of around 2000 laser shots. Mass spectra acquired in the reflector mode allowed detection of monoisotopic masses. External calibration using a dedicated peptide calibration mixture (AB Sciex), provided mass accuracy below 75 ppm. Data were processed using DataExplorer 4.9 software. The MS/MS experiments reported in this study were performed without use of a collision gas. Native LOS samples were prepared as previously reported.[34]

Acknowledgements

A.S. and A.M. acknowledge the TOLLerant H2020-MSC-ETN-642157 (http://www.tollerant.eu) project.

Conflict of Interest

The authors declare no conflict of interest.

Keywords: *bradyrhizobium* ORS285 · lipooligosaccharides · mass spectrometry · NMR spectroscopy · symbiosis

[1] C. Masson-Boivin, E. Giraud, X. Perret, J. Batut, *Trends Microbiol.* **2009**, *17*, 458–466.
[2] H. Ogutcu, A. Adiguzel, M. Gulluce, M. Karadayi F. Sahin, *Rom. Biotech. Lett.* **2009**, *14*, 4294–4300.
[3] E. Giraud, L. Moulin, D. Vallenet, V. Barbe, E. Cytryn, J. C. Avarre, M. Jaubert, D. Simon, F. Cartieaux, Y. Prin, G. Bena, L. Hannibal, J. Fardoux, M. Kojadinovic, L. Vuillet, A. Lajus, S. Cruveiller, Z. Rouy, S. Mangenot, B. Segurens, C. Dossat, W. L. Franck, W.-S. Chang, E. Saunders, D. Bruce, P. Richardson, P. Normand, B. Dreyfus, D. Pignol, G. Stacey, D. Emerich, A. Vermeglio, C. Medigue, M. Sadowsky, *Science* **2007**, *316*, 1307–1312.
[4] N. Fraysse, F. Couderc, V. Poinsot, *Eur. J. Biochem.* **2003**, *270*, 1365–1380.
[5] M. A. Newman, J. M. Dow, A. Molinaro, M. Parrilli, *J. Endotoxin Res.* **2007**, *13*, 69–84.
[6] C. R. Raetz, C. Whitfield, *Annu. Rev. Biochem.* **2002**, *71*, 635–700.
[7] F. Di Lorenzo, C. De Castro, R. Lanzetta, M. Parrilli, A. Silipo, A. Molinaro in *Carbohydrates in Drug Design and Discovery* (Eds.: J. Jimenez-Barbero, F. J. Canada, S. Martin-Santamaria), RSC Publishing, London, **2015**, 38–63.
[8] A. Molinaro, O. Holst, F. Di Lorenzo, M. Callaghan, A. Nurisso, G. D'Errico, A. Zamyatina, F. Peri, R. Berisio, R. Jerala, J. Jiménez-Barbero, A. Silipo, S. Martín-Santamaría, *Chem. Eur. J.* **2015**, *21*, 500–519.
[9] a) A. Silipo, G. Vitiello, D. Gully, L. Sturiale, C. Chaintreuil, J. Fardoux, D. Gargani, H.-I. Lee, G. Kulkarni, N. Busset, R. Marchetti, A. Palmigiano, H. Moll, R. Engel, R. Lanzetta, L. Paduano, M. Parrilli, W.-S. Chang, O. Holst, D. K. Newman, D. Garozzo, G. D'Errico, E. Giraud, A. Molinaro, *Nat. Commun.* **2014**, *5*, 5106; b) I. Komaniecka, A. Choma, A. Mazur, K. A. Duda, B. Lindner, D. Schwudke, O. Holst, *J. Biol. Chem.* **2014**, *289*, 35644–35655.
[10] I. Lerouge, J. Vanderleyden, *FEMS Microbiol. Rev.* **2002**, *26*, 17–47.
[11] R. W. Carlson, L. S. Forsberg, E. L. Kannenberg, *Subcell. Biochem.* **2010**, *53*, 339–386.
[12] a) A. Silipo, M. R. Leone, G. Erbs, R. Lanzetta, M. Parrilli, W.-S. Chang, M.-A. Newman, A. Molinaro, *Angew. Chem. Int. Ed.* **2011**, *50*, 12610–12612; *Angew. Chem.* **2011**, *50*, 12818–12820; b) W. Li, A. Silipo, L. B. Gersby, M.-A. Newman, A. Molinaro, B. Yu, *Angew. Chem. Int. Ed.* **2017**, *56*, 2092–2096; *Angew. Chem.* **2017**, *129*, 2124–2128.
[13] K. Bonaldi, D. Gargani, Y. Prin, J. Fardoux, D. Gully, N. Nouwen, S. Goormachtig, E. Giraud, *Mol. Plant-Microbe Interact.* **2011**, *24*, 1359–1371.
[14] N. Busset, A. De Felice, C. Chaintreuil, D. Gully, J. Fardoux, S. Romdhane, A. Molinaro, A. Silipo, E. Giraud, *PLoS One* **2016**, *11*, e0148884.
[15] J.-G. Noh, H.-E. Jeon, J.-S. So, W.-S. Chang, *Int. J. Mol. Sci.* **2015**, *16*, 16778–16791.
[16] R. W. Carlson, S. Kalembasa, D. Turowski, P. Pachori, K. D. Noel, *J. Bacteriol.* **1987**, *169*, 4923–4928.
[17] K. D. Noel, L. S. Forsberg, R. W. Carlson, *J. Bacteriol.* **2000**, *182*, 5317–5324.
[18] C. De Castro, A. Molinaro, R. Lanzetta, A. Silipo, M. Parrilli, *Carbohydr. Res.* **2008**, *343*, 1924–1933.
[19] L. S. Forsberg, R. W. Carlson, *J. Biol. Chem.* **1998**, *273*, 2747–2757.
[20] A. Turska-Szewczuk, R. Russa, M. A. Karaś, W. Danikiewicz, G. Spólnik, *Carbohydr. Res.* **2015**, *409*, 1–8.
[21] B. L. Ridley, B. S. Jeyaretnam, R. W. Carlson, *Glycobiology* **2000**, *10*, 1013–1023.

[22] A. Muszyński, M. Laus, J. W. Kijne, R. W. Carlson, *Glycobiology* **2011**, *21*, 55 – 68.
[23] O. Westphal, K. Jann, *Carbohydr. Chem.* **1965**, *5*, 83 – 91.
[24] R. Kittelberger, F. Hilbink, *J. Biochem. Biophys. Methods* **1993**, *26*, 81 – 86.
[25] K. Leontein, B. Lindberg, J. Lönngren, *Methods Carbohydr. Chem.* **1978**, *62*, 359 – 362.
[26] C. De Castro, M. Parrilli, O. Holst, A. Molinaro, *Methods Enzymol.* **2010**, *480*, 89 – 115.
[27] I. Ciucanu, F. Kerek, *Carbohydr. Res.* **1984**, *131*, 209 – 217.
[28] E. T. Rietschel, *Eur. J. Biochem.* **1976**, *64*, 423 – 428.
[29] J. P. Young, H. L. Downer, B. D. Eardly, *J. Bacteriol.* **1991**, *173*, 2271 – 2277.
[30] A. Silipo, S. Leone, A. Molinaro, R. Lanzetta, M. Parrilli, *Carbohydr. Res.* **2004**, *339*, 2241 – 2248.
[31] O. Holst, J. E. Thomas-Oates, H. Brade, *Eur. J. Biochem.* **1994**, *222*, 183 – 194.
[32] L. Sturiale, D. Garozzo, A. Silipo, R. Lanzetta, M. Parrilli, A. Molinaro, *Rapid Commun. Mass Spectrom.* **2005**, *19*, 1829 – 1834.
[33] B. W. Gibson, J. J. Engstrom, C. M. John, W. Hines, A. M. Falick, *J. Am. Soc. Mass Spectrom.* **1997**, *8*, 645 – 658.
[34] L. Sturiale, A. Palmigiano, A. Silipo, Y. A. Knirel, A. P. Anisimov, R. Lanzetta, M. Parrilli, A. Molinaro, D. Garozzo, *J. Mass. Spectrom.* **2011**, *46*, 1135 – 1142.
[35] J. W. Kloepper, C. J. Beauchamp, *Can. J. Microbiol.* **1992**, *38*, 1219 – 1232.
[36] G. Kato, Y. Maruyama, M. Nakamura, *Agric. Biol. Chem.* **1980**, *44*, 2843 – 2855.
[37] R. W. Carlson, B. S. Krishnaiah, *Carbohydr. Res.* **1992**, *231*, 205 – 219.
[38] R. W. Carlson, B. Reuhs, T. B. Chen, U. R. Bhat, K. D. Noel, *J. Biol. Chem.* **1995**, *270*, 11783 – 11788.
[39] E. L. Kannenberg, R. W. Carlson, *Mol. Microbiol.* **2001**, *39*, 379 – 391.
[40] L. Wang, Q. Wang, P. R. Reeves, *Subcell Biochem.* **2010**, *53*, 123 – 152.
[41] C. Galanos, O. Lüderitz, O. Westphal, *Eur. J. Biochem.* **1969**, *9*, 245 – 249.
[42] U. Piantini, O. W. Sorensen, R. R. Ernst, *J. Am. Chem. Soc.* **1982**, *104*, 6800 – 6801.
[43] M. Rance, O. W. Sorensen, G. Bodenhausen, G. Wagner, R. R. Ernst, K. Wüthrich, *Biochem. Biophys. Res. Commun.* **1983**, *117*, 479 – 485.
[44] D. J. States, R. A. Haberkorn, D. J. Ruben, *J. Magn. Reson.* **1982**, *48*, 286 – 292.
[45] A. S. Stern, K. B. Li, J. C. Hoch, *J. Am. Chem. Soc.* **2002**, *124*, 1982 – 1993.

Received: April 7, 2017
Version of record online June 12, 2017

